Journal of Nonlinear Optical Physics & Materials
Vol. 16, No. 2 (2007) 185–198

World Scientific
www.worldscientific.com

MULTIPLE QUASI-PHASE MATCHING IN ENGINEERED DOMAIN-INVERTED OPTICAL SUPERLATTICE

MING LU and XIANFENG CHEN*

Department of Physics, The State Key Laboratory on Fiber Optic Local Area Communication Networks and Advanced Optical Communication Systems, Shanghai Jiao Tong University, 800, Dong Chuan Road, Shanghai, 200240, China
**xfchen@sjtu.edu.cn*

Received 23 May 2007

With the emergence of engineered domain-inverted optical superlattices in recent years, multiple quasi-phase-matching (QPM) can be achieved in a single chip crystal, and has wide applications in frequency conversion. Of late, some approaches have been proposed in constructing a domain-inverted optical superlattice in order to implement multiple QPM. This paper briefly reviews the development of multiple QPM, and introduces main applications and new approaches in this field.

Keywords: Multiple QPM; optical superlattice; parametric process.

1. Introduction

Nonlinear crystal designs which exploit quasi-phase-matching (QPM) can achieve considerable control over the wavelength conversion efficiency by modifying the structure of the nonlinear crystal.[1] QPM is widely used for optical parametric processes because of its largest usable nonlinear optical coefficient and a wider range of phase-matchable wavelengths compared with those of the conventional birefringence phase-matching techniques.[2–3] With the development of room temperature poling technology, it is possible to achieve domain-inverting structures in ferroelectric crystals such as $LiNbO_3$, $LiTaO_3$, $KTiOPO_4$ and so on.[4–13] QPM uses modulation of the nonlinear coefficient of the crystal to compensate for the mismatch between the wave vectors of the interacting light beams. Therefore, it substantially extends the class of materials available to various nonlinear optical interactions.[14–17] The first kind of optical supperlattice is the periodic optical superlattice (POS), with a periodic domain-inverting structure. POS has been widely utilized in $\mathrm{LiTaO_3}$,[18,19] $\mathrm{LiNbO_3}$,[20–25] KTP[26] and other ferroelectric crystals.[27,28]

POS can provide only one reciprocal vector to compensate for the wave-vector mismatch in a given nonlinear optical process, and has a narrow acceptance bandwidth for pump wavelength and operating temperature. In order to solve these problems, the multiple QPM optical superlattice was proposed, which can provide more reciprocal vectors to realize multiple parametric processes simultaneously.

2. One-Dimensional QPM

2.1. *Quasi-periodical optical superlattice (QPOS)*

In 1997, a nonlinear optical superlattice of $LiTaO_3$ was designed and fabricated, in which two anti-parallel 180± domain building blocks A and B were arranged as a Fibonacci sequence.[29] This structure is named Quasi-periodic optical superlattice (QPOS), which can provide more reciprocal vectors to satisfy multi-quasi-phase-matching processes simultaneously than POS. The QPOS can be fabricated using the pulse field poling technique at room temperature. The phase matching condition in the second harmonic process of a QPOS can be written as $\Delta k = k_{2\omega} - 2k_\omega - G_{m,n} = 0$, where $k_{2\omega}, k_\omega$ are the wave vectors of the second harmonic and fundamental wave, respectively, and $G_{m,n}$ is the reciprocal vector which depends on the structure parameter. The second harmonic spectrum of QPOS has been studied theoretically, and experimental realization of multiple wavelength second-harmonic generation (SHG) is reported, with the conversion efficiencies comparable with those of a POS. The results show that the QPOS may be applied to some multiple wavelength SHG devices. Because more reciprocal vectors can be provided by a QPOS, not only the multiple QPM SHG, but also some coupled parametric processes, such as the third-harmonic generation (THG) and fourth-harmonic generation (FHG), can be realized with high efficiency. In the same year, for the first time, direct THG was gained with high efficiency by one Fibonacci QPOS based on $LiTaO_3$.[30] As is shown in Fig. 1, for a Fibonacci QPOS, the QPM conditions for THG are $\Delta k_1 = k_{2\omega} - 2k_\omega - G_{m,n} = 0$ for SHG and $\Delta k_2 = k_{3\omega} - k_{2\omega} - k_\omega - G_{m',n'} = 0$ for SFG.

$G_{m,n}$ and $G_{m',n'}$ are two different pre-designed reciprocal vectors of the QPOS in Fibonacci sequences. The QPOS can provide two specially designed reciprocal vectors: $G_{m,n}$ is used to compensate the mismatch of wave vectors in the SHG process, and $G_{m',n'}$ is used to compensate the mismatch of wave vectors in the SFG process. Two QPM conditions, $\Delta k_1 = 0$ and $\Delta k_2 = 0$, are simultaneously satisfied in the coupled parametric process, which leads to a THG with high efficiency.

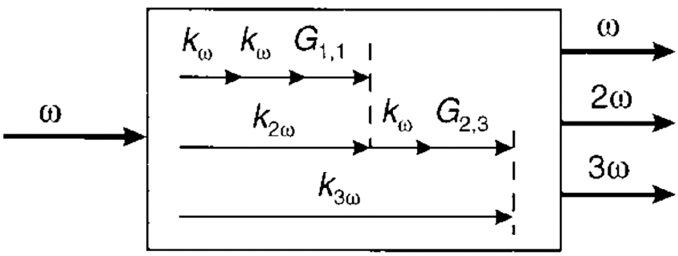

Fig. 1. Schematic diagram of the process of THG in a QPOS material.[30]

Other QPOSs were proposed to meet different multiple QPM processes, such as three-element Fibonacci structure and Thue-Morse structure[31] and so on.

2.2. *Aperiodic optical superlattice (AOS)*

One question naturally raised is whether the QPOS with Fibonacci sequence is the best candidate for nonlinear optical processes. An aperiodic optical superlattice (AOS) is proposed in which the periodicity of the structure disappears. There are two ways to construct an AOS, one is by optimization algorithms, another is by modulation of the periodic structure. Theoretically, AOS contains more plentiful Fourier spectral components than those in the QPOS, therefore, it can provide more reciprocal vectors. Thus, it may be expected that the AOS can become another favorable candidate for optical parametric devices.

2.2.1. *AOS designed by optimization algorithms*

The design of the AOS by optimization algorithms corresponds to an inverse source problem in nonlinear optics.[32] In this method, the crystal with total length L is divided into N unit blocks with congruent length ΔL, and the polarization direction of each block is upwards or downwards, described by the function $d(z) = d_{33} \cdot g(z)$, when the largest nonlinear coefficient d_{33} is used. $g(z)$ is the function taking binary values of 1 or -1. Taking multiple SHG as an example and considering the small-signal and slowly varying approximation, the pump depletion and transmission loss not taken into account, the amplitude of the SHG wave produced is:

$$A_{2\omega} = i\frac{2\omega}{n_{2\omega}c}A_\omega^2 \int_o^L d(z)\exp[-i\Delta k(\lambda)z]dz = i\frac{2\omega}{n_{2\omega}c}A_\omega^2 G(\lambda) \tag{1}$$

$$G(\lambda) = \int_o^L d(z)\exp[-i\Delta k(\lambda)z]dz. \tag{2}$$

The conversion efficiency η from fundamental wave to second harmonics reads

$$\eta = \frac{8\pi^2 \left|d_{33}\right|^2 I_\omega L^2}{c\varepsilon_0 \lambda^2 n_{2\omega} n_\omega^2} \left|\frac{1}{L}\int_o^L g(z)\exp[-i\Delta k(\lambda)z]dz\right|, \tag{3}$$

where $n_\omega(n_{2\omega})$ is the index of refraction of the fundamental (second harmonics) wave, c is the speed of light in vacuum, λ is the wavelength of the fundamental light in vacuum, ε_0 is the dielectric constant in vacuum, and g(z) represents the orientation of each block taking binary values of 1 or -1. $\Delta k(\lambda) = k_{2\omega} - 2k_w$ presents the phase mismatch between the fundamental wave and second harmonics, where $k_\omega(k_{2\omega})$ is the wavevector of the fundamental (second harmonics) wave. $g(z)$ is optimized by optimization algorithms. The first AOS structure realized by inverting poled ferroelectric domains was reported in 1999, optimized by the simulated annealing algorithm,[33] as is shown in Fig. 2. The constructed AOS can implement

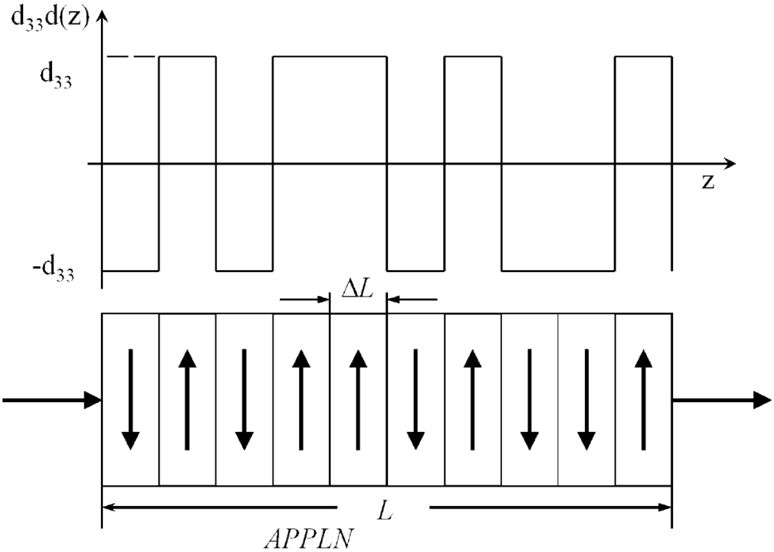

Fig. 2. Schematic diagram of AOS.

multiple wavelengths second-harmonic generation and the coupled third-harmonic generation with an identical effective nonlinear coefficient. The numerical simulations show that the constructed AOS can enhance harmonic generation compared with the Fibonacci optical superlattice. The influence of the random fluctuation of the thickness of blocks on the performance of the constructed AOSs is also investigated in detail for simulating practical fabrications.[34]

As we know, the conversion efficiency increases quadratically with the interaction length, while the bandwidth scales inversely with the length. But the narrow acceptance bandwidth for the fundamental wavelength and temperature, which exceeds the tolerances on laser diodes due to the fluctuation of laser wavelength or temperature, or due to errors in the fabrication process, critically limits the utility of the QPM technique.[35] The approach to obtain wide flattop bandwidth based on aperiodic domain-inverted gratings is proposed.[36] The sequences and the length of the domains are optimized to realize the pre-designed wide bandwidth by the simulated annealing (SA) method.

In summary, AOS can supply much more reciprocal vectors for multiple QPM and implement pre-designed flattop response with the optimum sequence. It has been employed to achieve QPM multiple and broaden-band wavelength conversion in the past.[37,38]

In order to gain higher conversion efficiency and more flexible design, new approaches were made based on AOS.[39–41] An effective approach for designing the AOS to separately achieve parametric amplification of multiple discrete wavelengths is presented, with identical amplification coefficient at the prescribed wavelengths of signal light.[39] Using a similar approach, a new technique is described for designing

QPM gratings which allows the SHG frequency response of a grating to be tailored to any desired profile using a combination of analytic and numerical methods.[40]

In 2007, a new algorithm called the self-adjusting algorithm is proposed to construct the AOS,[41] in which multiple nonlinear optical parametric processes can be realized simultaneously with high conversion efficiency in an extremely short time, which is shown in Fig. 3.

Figure 3 shows the initial result without feedback optimization (a), the result after one optimizing step (b) and the result after seven optimizing steps (c), respectively. The four peak values at the designed wavelength after every step of optimizing are shown in (d). After three steps, the four peak values are very close to each other. After seven steps, four peaks with identical effective nonlinear coefficients of 0.229 at the designed wavelengths are found. Considering the effective nonlinear coefficient of QPM SHG as a function of fundamental wavelength in AOS structure optimized by the self-adjusting algorithm with $N = 3000$ and $\Delta L = 3.3\,\mu\text{m}$, the designed wavelengths are 1060 nm, 1082 nm, 1283 nm, 1364 nm, respectively.

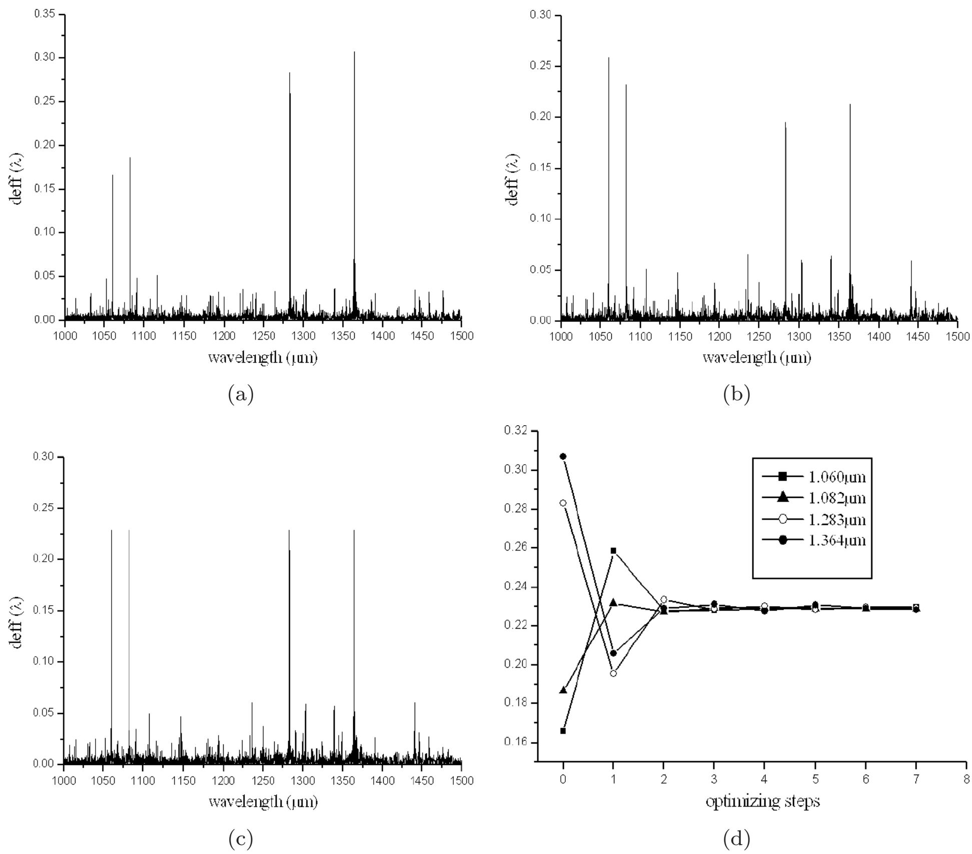

Fig. 3. The calculation results by self-adjusting algorithm.[41]

The self-adjusting algorithm is based on the physical principle of the specific nonlinear optical process, and uses a feedback function to avoid huge amounts of tentative and repeating calculations, so that the calculation time is much shorter than using other optimization algorithms which exist, such as simulated annealing algorithm (SA), genetic algorithm (GA), and so on. Besides, the self-adjusting algorithm is independent of initial condition, so it is proven to be a more flexible and effective algorithm to construct ideal AOS for multiple QPM processes.

2.2.2. *AOS designed by modulation of periodic structure*

The range of reciprocal vectors can be increased by perturbing the periodic structure, so that spectral components in wavevector domains can spread to the wings. This method is widely used to broaden the phase matching bandwidth in QPM SHG devices. Phase-shifted gratings,[42] phase-reversal sequence (PRS) technique,[43] segmented grating[44–47] and other schemes have been proposed and investigated. Segmented grating makes use of located phase shifts inserted into a periodic grating, as is shown in Fig. 4. The segmented QPM grating is supposed to be fabricated in a Z-cut and X-propagating nonlinear crystal and consists of N segments. The device total length is L. The length and the period of each segment are L_i and Λ_i $(i = 1, 2, \ldots, N)$. For segment m, the couple equations are expressed as[48]

$$\frac{dA_{1m}}{dx} = -j\kappa A_{1m}^{*} A_{2m} e^{-j\Delta\Phi_m}$$

$$\frac{dA_{2m}}{dx} = -j\kappa A_{1m}^{2} e^{j\Delta\Phi_m}, \tag{4}$$

where A_1 and A_2 denote the amplitudes of the fundamental signal and the second harmonic respectively. κ is the nonlinear coefficient, and $\Delta\Phi_m$ is the phase mismatch in segment m.

For segmented gratings, the QPM conditions are easily satisfied in relatively wider laser wavelengths and a larger temperature region because of the enhancement of bandwidth and temperature tolerance. The requirement of laser source stability

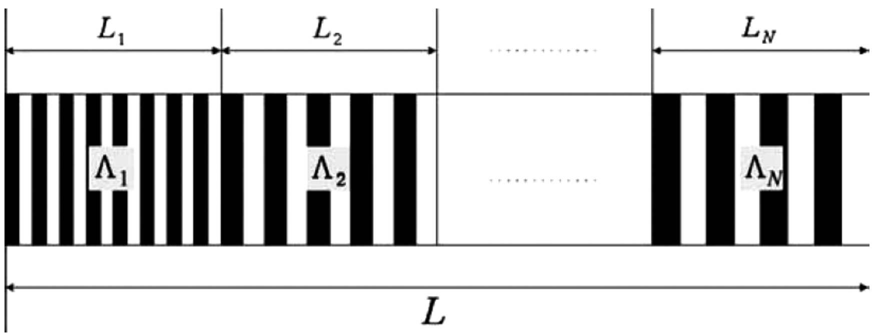

Fig. 4. Schematic description of the segmented QPM grating.[48]

and environment temperature accuracy is greatly reduced. The greater the number of segments, the broader the conversion bandwidth and temperature tolerance are, however, the lower the conversion efficiency is.

Segmented gratings structure requires fine adjustment of the period and the phase shifts. Many schemes have been demonstrated to broaden the bandwidth by chirping grating periods.[49–51] The physical origin of the bandwidth enhancement is ascribed to the plentiful reciprocal vectors provided by the chirping grating periods. The linearly chirped grating period is

$$\Lambda(x) = \frac{\Lambda_0}{1 + (x - x_{QPM})}, \tag{5}$$

where $\Lambda_0 = 2\pi/(k_{2\omega} - 2k_\omega)$ is the periodic QPM grating period, x_{QPM} is the position of the exact phase matching point, and r is the chirp coefficient. The linearly chirped grating is illustrated in Fig. 5, when the chirp coefficient $r < 0$ and $r > 0$, respectively.

A broadband wavelength converter based on linearly chirped gratings in $LiNbO_3$ crystal has been reported.[52] The wavelength converter provides broader bandwidth than that based on periodic gratings, which are commonly used for wavelength conversion.

Other chirping grating periods, such as sinusoidally chirped optical superlattice (SCOS), are proposed.[53,54] For the SCOS, the period is expressed as

$$\Lambda(x) = \frac{\Lambda_0}{1 + \sin\frac{2N\pi x}{L} + \frac{2N\pi x}{L}\cos\frac{2N\pi x}{L}}, \tag{6}$$

where r is the chirp coefficient, L is the device length, N is the period number of the sine function, $\Lambda_0 = 2\pi/(k_{2\omega} - 2k_\omega)$ is the periodic QPM grating period. The SCOS is schematically described in Fig. 6.[54]

Compared with segmented gratings and linearly chirped grating, SCOS will greatly broaden the bandwidth and flatten the response, because more plentiful

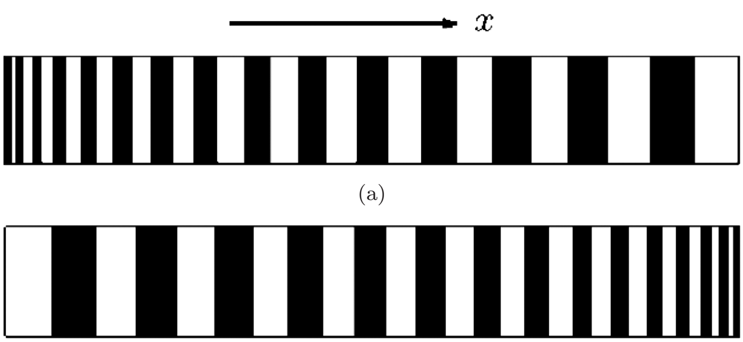

Fig. 5. Schematic description of linearly chirped gratings. (a) Chirp coefficient $r < 0$; (b) chirp coefficient $r > 0$.[52]

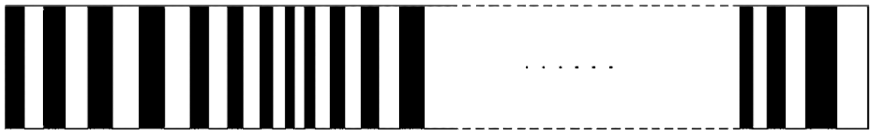

Fig. 6. Schematic description of the SCOS structure.[54]

and flexible reciprocal wave vectors can be provided by SCOS. Difference-frequency generation (DFG)-based wavelength conversion with (SCOS) is also reported.

2.3. *Nonperiodic optical superlattice (NOS)*

In the AOS theory, in order to achieve a pre-designed multiple QPM process, samples are divided into blocks with congruent length. The spontaneous polarization direction of each block is determined by optimization algorithms. Although the periodicity of domain inversion disappears in AOS, each block must be of one or multiple fixed lengths. Therefore it is naturally expected that the arbitrary domain length of a block in the optical superlattice will provide an even greater number of flexible reciprocal vectors for QPM nonlinear optical processes than the AOS. A new optical superlattice: nonperiodic optical superlattice (NOS) is proposed, in which the limitation to block length disappears.[55] In this paper, an ideal construction of NOS for predesigned multiple QPM SHG processes is achieved by the combination of stimulated annealing (SA) and genetic algorithm methods, as shown in Fig. 7. Another scheme for constructing NOS is also reported,[56] by which direct THG and other multiple QPM processes can be generated with high efficiency. The numerical simulations show that NOS can be used as a more effective and useful nonlinear optical crystal for multiple nonlinear optical parametric generation.

3. Two-Dimensional QPM Techniques

1-dimensional (1-D) optical superlattice has been investigated in recent year. In 1998, V. Berger proposed extending the idea of QPM to multiple spatial dimensions in much the same way as conventional linear gratings have been extended to photonic crystals(PC),[57] as is shown in Fig. 8.

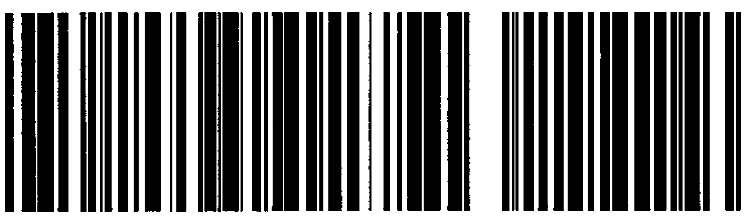

Fig. 7. Gray-scale diagram of the NOS in part.[56]

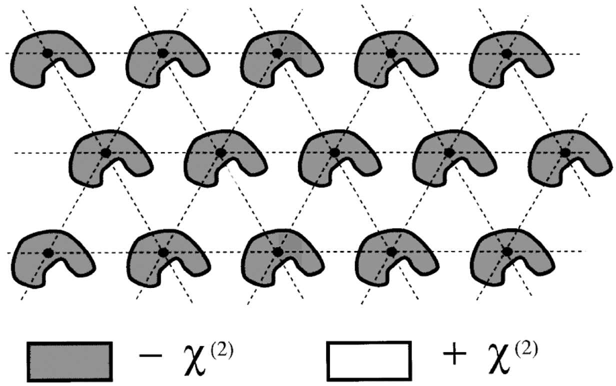

Fig. 8. Schematic picture of a 2-D optical superlattice.[57]

As the fabrication of a 3-D optical superlattice seems to be very tricky, recent investigations mainly concentrate on the 2-D optical superlattice. In such a nonlinear photonic crystal (NPC) there is a spatial variation of a nonlinear susceptibility tensor while the refractive index is constant. The QPM condition appears as the expression of the momentum conservation in such a NPC, for example, as a QPM SHG process: $\vec{k}_{2\omega} - 2\vec{k}_{\omega} - \vec{G} = 0$, where $\vec{G}$ is the 2-D reciprocal vectors provided by a 2-D optical superlattice, and generally, $\vec{k}_{2\omega}$ and $\vec{k}_{\omega}$ are not parallel to each other, as is shown in Fig. 9. Theoretically, reciprocal vectors will be provided by the 2-D optical superlattice to satisfy multiple QPM processes simultaneously.[57]

Like the development of 1-D QPM, nonlinear frequency conversion in the 2-D periodic optical superlattice (2DPOS) was first studied.[58–63] It is shown that these

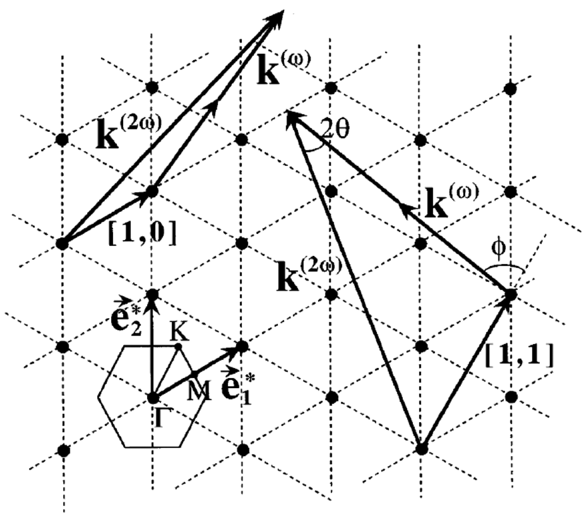

Fig. 9. Reciprocal vectors and QPM process in 2-D periodic hexagonal lattice.[57]

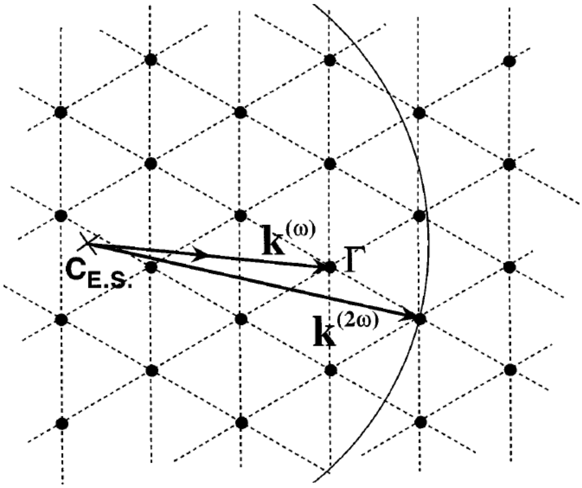

Fig. 10. Nonlinear Ewald construction in 2-D periodic hexagonal lattice.[57]

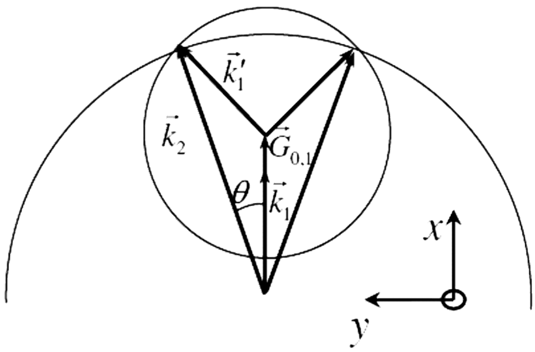

(a)

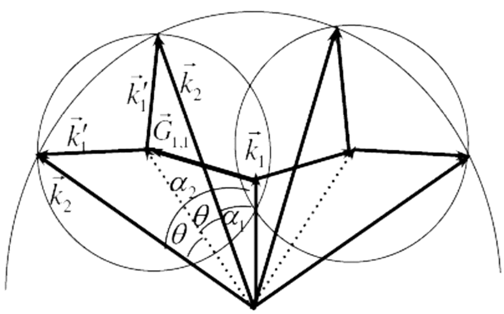

(b)

Fig. 11. Phase-matching geometries for (a) the axially symmetrical ring and (b) the mirror-symmetrical rings.[63]

in-plane phase-matching resonances are given by a nonlinear Bragg law, and a related nonlinear Ewald construction, as is shown in Fig. 10.[57] Applications such as multiple-beam second-harmonic generation (SHG), ring cavity SHG, or multiple wavelength frequency conversion are envisaged.

The 2DPOS fabricated by field poling technique was reported,[58] with a periodic hexagonal lattice, in which QPM is obtained for multiple directions of propagation with internal conversion efficiencies of 80%.

A new type of conical second-harmonic generation was discovered in a 2DPOS: a hexagonally poled $LiTaO_3$ crystal, and it reveals the presence of another type of nonlinear interaction: a scattering involving optical parametric generation in a nonlinear medium.[63] Such a nonlinear interaction can be significantly enlarged in a modulated $\chi^{(2)}$ structure by a QPM process, as is shown in Fig. 11. The conical beam records the spatial distribution of the scattering signal and discloses the structure information and symmetry of the 2D $\chi^{(2)}$ photonic crystal.

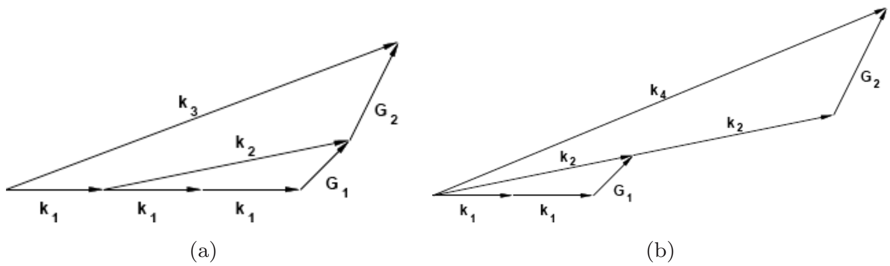

Fig. 12. Generic QPM schemes for (a) THG, (b) FHG. Reciprocal lattice vectors G_1 and G_2 phase match quadratic interactions between jth harmonic wave vectors k_j.[64]

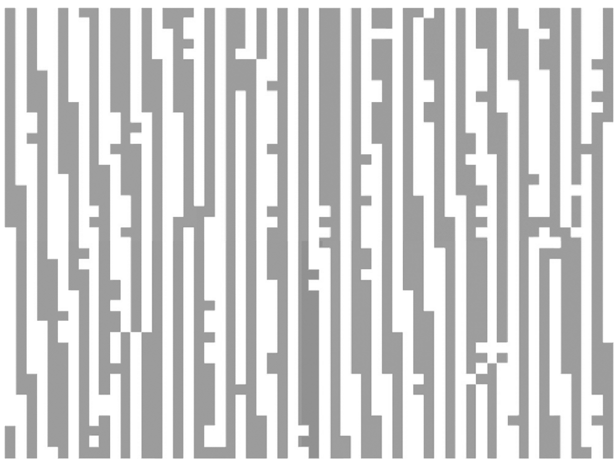

Fig. 13. A gray-scale diagram of the constructed 2DAOS in part. The black(white) blocks represent the positive(negative) domains.[65]

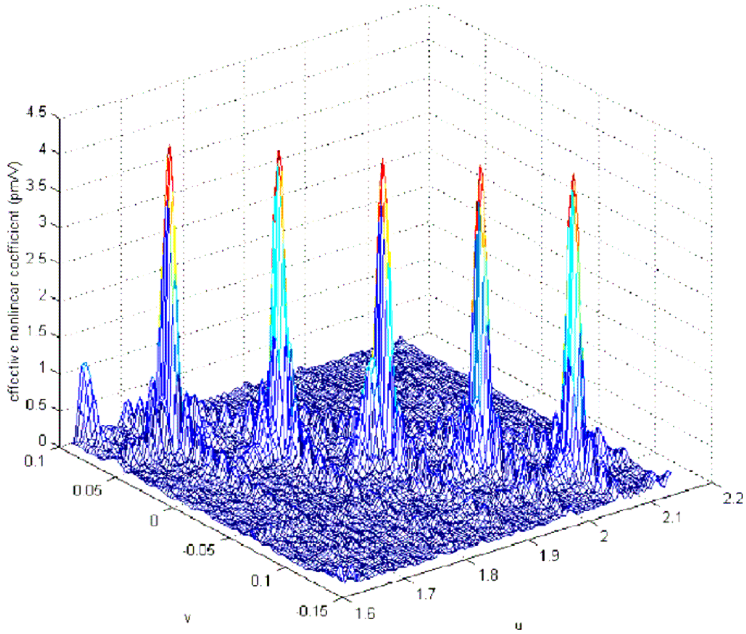

Fig. 14. Effective nonlinear coefficient in the constructed 2DAOS, the calculated peak value of effective nonlinear coefficient at the five given fundamental wavelengths is about 3.8 pm/V.[65]

THG and FHG were also studied in the 2DPOS.[64] Reciprocal vectors were provided by designed patterns to compensate for the phase mismatch among the wave vectors involved in the THG and FHG processes, as is shown in Fig. 12, which leads to THG and FHG with high conversion efficiency theoretically.

2DPOS extends the applications of the QPM technique and provides a new kind of nonlinear optical crystal for various frequency conversion applications by nonlinear optical processes. It can be naturally expected that a 2-dimensional aperiodic optical superlattice (2DAOS), evolving from 1DAOS and 2DPOS, may realize even more flexible QPM conditions in comparison with currently suggested approaches.[65] The structure of the first 2DAOS is designed to implement multiple SHG with identical effective nonlinear coefficient by SA algorithm, Fig. 13 and Fig. 14. It is shown that 2DAOS can expand the applications of QPM techniques and will be a new nonlinear optical material for the optical frequency conversion process.

4. Conclusions

Engineered structures of optical superlattice are introduced to expand the amount of the requisite superlattice reciprocal vectors greatly and make the multiple QPM available in recent years. Advancements were made from a 1-dimensional to 2-dimensional structure, and from POS to QPOS (quasi-periodic optical superlattice), to AOS (aperiodic optical superlattice), to NOS (nonperiodic optical superlattice) and other complex structures. The multiple frequency conversion based on the multiple QPM schedule shows potential applications in nonlinear optics for laser sources and optical information.

Acknowledgments

This research was supported by the National Natural Science Foundation of China (No. 60477016 and No.10574092) and the National Basic Research Program "973" of China (2006CB806000).

References

1. J. A. Armstrong, N. Bloembergen, J. Ducuing and P. S. Pershan, *Phys. Rev.* **127** (1962) 1918.
2. L. E. Myers, R. C. Eckardt, M. M. Fejer, R. L. Byer, W. R. Bosenberg and J. W. Pierce, *J. Opt. Soc. Am. B* **12** (1995) 2102.
3. Shoji, T. Kondo, A. Kitamoto, M. Shiraneand and R. Ito, *J. Opt. Soc. Am. B* **14** (1997) 2268.
4. S. Miyazawa and J. C. Peuzin, *Appl. Phys. Lett.* **48** (1986) 1104.
5. M. Yamada, N. Nada, M. Saitoh and K. Watanabe, *Appl. Phys. Lett.* **62**(5) (1993) 435.
6. S. N. Zhu, Y. Y. Zhu, Z. Y. Zhang, H. Shu, H. F. Wang, J. F. Hong and C. Z. Ge, *J. Appl. Phys.* **77**(IO) (1995) 15.
7. S. Somkeh and A. Yariv, *Opt. Commun.* **6** (1972) 301.
8. D. Feng *et al.*, *Appl. Phys. Lett.* **37** (1980) 607.
9. R. L. Byer, *Nonlinear Opt.* **7** (1994) 234.
10. V. Pruneri, J. Webjorn, J. Russell, D. C. Hanna, *Appl. Phys. Lett.* **65** (1995) 2126.
11. H. Ito, C. Takyu and H. Inaba, *Electron. Lett.* **27** (1991) 1221.
12. M. C. Gupta, W. Kozlovesky and A. C. G. Nutt, *Appl. Phys. Lett.* **64** (1994) 3210.
13. J. D. Bierlein *et al.*, ibid. **56** (1990) 1725.
14. J. Webjorn, F. Laurell and G. Arvidsson, *J. Lightwave Technol.* **7** (1989) 1597.
15. M. M. Fejer, G. A. Magel, D. H. Jundt and R. L. Byer, *IEEE J. Quantum Electron.* **28** (1992) 2631.
16. V. Pruneri, R. Koch, P. G. Kazansky, W. A. Clarkson, P. St. J. Russell and D. C. Hanna, *Opt. Lett.* **20** (1995) 2375.
17. G. D. Miller, R. G. Batchko, W. M. Tulloch, D. R. Weise, M. M. Fejer and R. L. Byer, *Opt. Lett.* **22** (1997) 1834.
18. K. Mizuuchi and K. Yamamoto, *Appl. Phys. Lett.* **60** (1992) 1283.
19. J. P. Meyn and M. M. Fejer, *Opt. Lett.* **22** (1997) 1214.
20. M. H. Chou, J. Hauden, M. A. Arbore and M. M. Fejer, *Opt. Lett.* **23** (1998) 104.
21. M. H. Chou, I. Brener, M. M. Fejer, E. E. Chaban and S. B. Christman, *IEEE Photonic. Tech. Lett.* **11** (1999) 653.
22. K. R. Parameswaran, J. R. Kurz, R. V. Roussev and M. M. Fejer, *Opt. Lett.* **27** (2002) 43.
23. C. Q. Xu, H. Okayama and M. Kawahara, *Appl. Phys. Lett.* **63** (1993) 3559.
24. M. H. Chou, J. Hauden, M. A. Arbore and M. M. Fejer, *Opt. Lett.* **23** (1998) 1004.
25. M. H. Chou, K. R. Parameswaran, M. A. Arbore, J. Hauden and M. M. Fejer, Bidirectional wavelength conversion between 1.3- and 1.5- m telecommunication bands using difference frequency mixing in $LiNbO_3$ waveguides with integrated coupling structures, in *Proc. Conference on Lasers and Electro-Optics*, Vol. 6 (Optical Society of America, Washington, D.C. 1998).
26. U. L. Andersen and P. Buchhave, *Opt. Express* **10** (2002) 887.
27. S. J. B. Yoo, *J. Lightwave Technol.* **14** (1996) 955.

28. H. Y. Chen, J. S. Sue, Y. H. Lin and S. Chao, *Opt. Lett.* **28** (2003) 917.
29. S. N. Zhu, Y. Y. Zhu, Y. Q. Qin, H. F. Wang, C. Z. Ge and N. B. Ming, *Phys. Rev. Lett.* **78** (1997) 2752.
30. S. N. Zhu, Y. Y. Zhu and N. B. Ming, *Science* **278** (1997) 843.
31. X. J. Liu *et al.*, *Chin. Phys. Lett.* **15** (1998) 426.
32. S. Kirkpatrick, C. D. Gelatt Jr. and M. P. Vecchi, *Science* **220** (4598) (1983) 671.
33. B. Y. Gu, B. Z. Dong, Y. Zhang and G. Z. Yang, *Appl. Phys. Lett.* **75** (1999) 2175.
34. B. Y. Gu, Y. Zhang and B. Z. Dong, *J. Appl. Phys.* **87** (2000) 7629.
35. M. L. Bortz, M. Fujimura and M. M. Ferjer, *Electron. Lett.* **30** (1994) 34.
36. X. L. Zeng, X. F. Chen, F. Wu, Y. P. Chen, Y. X. Xia and Y. L. Chen, *Opt. Commun.* **204** (2002) 407.
37. K. Gallo, G. Assanto and G. I. Stegeman, *Appl. Phys. Lett.* **71** (1997) 1020.
38. W. Xie, X. F. Chen , Y. P. Chen and Y. X. Xia, *Opt. Commun.* **251** (2005) 179.
39. Y. Zhang and B. Y. Gu, *Opt. Commun.* **192** (2001) 417.
40. D. T. Reid, *J. Opt. A: Pure and Appl. Opt.* **5** S(2003) 97.
41. M. Lu, *Appl. Opt.* in Press (2007).
42. K. Mizuuchi and K. Yamamoto, *Opt. Lett.* **23** (1998) 1880.
43. M. H. Chou, K. R. Parameswaran, M. M. Fejer and I. Brener, *Opt. Lett.* **24** (1999) 1157.
44. K. Mizuuchi, K. Yamamoto, M. Kato and H. Sato, *IEEE J. Quantum Electron.* **30** (1994) 1596.
45. X. Liu, H. Zhang, Y. Guo and Y. Li, *IEEE J. Quantum Electron.* **38** (2002) 1225.
46. Z. W. Liu, S. N. Zhu, Y. Y. Zhu, H. T. Wang, G. Z. Luo, H. Liu, N. B. Ming, X. Y. Liang and Z. Y. Xu, *Chin. Phys. Lett.* **18** (2001) 539.
47. S. M. Gao, C. X. Yang, X. S. Xiao and G. F. Jin, *Opt. Commun.* **233** (2004) 205.
48. T. Suhara and H. Nishihara, *IEEE J. Quantum Electron.* **26** (1990) 1265.
49. M. Asobe, O. Tadanaga, H. Miyazawa, Y. Nishida and H. Suzuki, *Opt. Lett.* **28** (2003) 558.
50. Y. W. Lee, F. C. Fan, Y. C. Huang, B. Y. Gu, B. Z. Dong and M. H. Chou, *Opt. Lett.* **27** (2002) 2191.
51. Bang, C. B. Clausen, P. L. Christiansen and L. Torner, *Opt. Lett.* **24** (1999) 1413.
52. S. M. Gao, C. X. Yang and G. F. Jin, *Chin. Phys. Lett.* **20** (2003) 1272.
53. S. M. Gao, C. X. Yang and G. F. Jin, *IEEE Photon. Technol. Lett.* **16** (2004) 557.
54. S. M. Gao, C. X. Yang and G. F. Jin, *Opt. Commun.* **239** (2004) 333.
55. X. F. Chen, F. Wu, X. L. Zeng, Y. P. Chen, Y. X. Xia and Y. L. Chen, *Phys. Rev. A* **69** (2004) 013818.
56. A. H. Norton and C. Martijn de Sterke, *Opt. Express* **12** (2004) 841.
57. V. Berger, *Phys. Rev. Lett.* **81** (1998) 4136.
58. N. G. R. Broderick, G. W. Ross, H. L. Offerhaus, D. J. Richardson and D. C. Hanna, *Phys. Rev. Lett.* **84** (2000) 4345.
59. Chowdhury, S. C. Hagness and L. McCaughan, *Opt. Lett.* **25** (2000) 832.
60. N. G. R. Broderick *et al.*, *J. Opt. Soc. Am. B* **19** (2002) 2263.
61. P. G. Ni, B. Q. Ma, X. H. Wang, B. Y. Cheng and D. Z. Zhang, *Appl. Phys. Lett.* **82** (2003) 4230.
62. L. H. Peng *et al.*, *Appl. Phys. Lett.* **83** (2003) 3447.
63. P. Xu, S. H. Ji, S. N. Zhu, X. Q. Yi, J. Sun, H. T. Wang, J. L. He, Y. Y. Zhu and N. B. Ming, *Phys. Rev. Lett.* **93** (2004) 133904.
64. H. Norton and C. M. de Sterke, *Opt. Express* **11** (2003) 1008.
65. L. J. Chen, X. F. Chen, Y. P. Chen and Y. X. Xia, *Phys. Lett. A* **349** (2006) 484.